Available online at www.sciencedirect.com
ScienceDirect
Progress in Oceanography 00 (2015) 1–??
Journal Logo

How important are coastal fronts to albacore tuna (*Thunnus alalunga*) habitat in the Northeast Pacific Ocean?

Karen Nieto[a,b], Yi Xu[a], Steven L. H. Teo[a], Sam McClatchie[a], John Holmes[c]

[a]*NOAA, Southwest Fisheries Science Center, 8901 La Jolla Shores Drive, La Jolla, CA 92037-1509, USA.*
[b]*European Commission, Joint Research Centre, Institute for Environment and Sustainability, Via E.Fermi, 2749, 21027, Ispra, VA, Italy.*
[c]*Fisheries and Oceans Canada, Pacific Biological Station, 3190 Hammond Bay Road, Nanaimo, B.C., V9T 6N7, Canada*

Abstract

We used satellite sea surface temperature (SST) data to characterize coastal fronts and then tested the effects of the fronts and other environmental variables on the distribution of the albacore tuna (*Thunnus alalunga*) catches in the coastal areas (from the coast to 200 nm offshore) of the Northeast Pacific Ocean. A boosted regression tree (BRT) model was used to explain the spatial and temporal patterns in albacore tuna catch per unit effort (CPUE) (1988-2011), using frontal features (distance to the front and temperature gradient), and other environmental variables like SST, surface chlorophyll concentration (chlorophyll), and geostrophic currents as explanatory variables. Based on over two decades of high-resolution data, the modeled results confirmed the previous findings that albacore CPUE distribution is strongly influenced by SST and chlorophyll at fishing locations, and the distance of fronts from the coast ($D_{FRONT-COAST}$), albeit with substantial seasonal and interannual variation. Albacore CPUEs were higher near warm, low chlorophyll oceanic waters, and near SST fronts. We performed sequential leave-one-year-out cross-validations for all years and found that the relationships in the BRT models were robust for the entire study period. Spatial distributions of model-predicted albacore CPUE were similar to observations, but the model was unable to predict very high CPUEs in some areas. These results help to explain previously observed variability in albacore CPUE and will likely help improve international fisheries management in the face of environmental changes.

Keywords: fishery oceanography, remote sensing, tuna fisheries, spatial variations, fronts, frontal features

1. Introduction

A major part of the albacore tuna (*Thunnus alalunga*) stock in the North Pacific is seasonally distributed along the coastal areas of the Northeast Pacific Ocean, where it supports important U.S. and Canadian fisheries. These coastal areas are part of the California Current System (CCS), which is one of five major eastern boundary current upwelling systems in the world ocean and extends from the bifurcation of the North Pacific Current (~50°N) to southern Baja California (~15–25°N). The CCS is usually classified into seven regions with boundaries at Cape Blanco, Cape Mendocino (~40°N), Point Reyes, Point Conception (~34°30′N), the Mexican-U.S. border, and Point Eugenia respectively (*Bernal*, 1979; *Thomas and Strub*, 2001). The CCS is characterized by seasonally variable wind forcing, and consequent summer upwelling near to the coast, especially between Cape Mendocino and Point Conception, and off northern Baja California. As a result of the upwelling, coastal fronts occur between the cold, near-shore water and warmer offshore water. Upwelling frontal systems exhibit instabilities that generate other mesoscale and submesoscale structures, such as filaments and eddies, depending on the width of the continental shelf and/or the presence of topographic discontinuities like capes.

Several previous studies have examined the effect of environmental variables on albacore distribution in the North-east Pacific (e.g., *Laurs et al.*, 1984; *Phillips*, 2011; *Phillips et al.*, 2014) but to the best of our knowledge, no previous

study has developed quantitative models on the effects of coastal frontal features on albacore distribution in the Northeast Pacific. Convergent flows associated with fronts can concentrate plankton and support a food web with large pelagic predators such as tunas at the top of the chain. The association between albacore tuna schools and fronts has been documented in different areas (*Fiedler and Bernard*, 1987; *Polovina et al.*, 2001; *Zainuddin et al.*, 2006; *Lan et al.*, 2012). *Fiedler and Bernard* (1987) analyzed the stomach contents of albacore caught off California and showed that they were feeding mainly on juvenile northern anchovy and that the distribution and diet of albacore was related to mesoscale fronts visible in satellite images of sea surface temperature (SST) and chlorophyll. Like other fish, albacore distribution near fronts in coastal areas may be related to a balance between the bioenergetics of maintaining appropriate body temperatures and increased food availability near these fronts (*Brandt*, 1993). *Laurs et al.* (1984) was the first to use satellite imaging to study albacore distribution in the Northeast Pacific and found that albacore were "located within pockets of warm, blue oceanic water intruding into the boundary between oceanic and cooler greenish coastal waters." *Brodeur et al*., (unpublished manuscript) applied a Generalized Additive Model to study the spatial and temporal variation in albacore habitat in the Northeast Pacific using monthly remotely sensed SST, chlorophyll, sea surface height, and wind stress curl from a 5-year time series (1999-2004). Their results suggested that albacore had a narrow habitat preference. *Phillips et al.* (2014) used a longer time series (1961-2008) and found that, at seasonal time scales, albacore catch per unit effort (CPUE) was primarily driven by SST, whereas at inter-annual scales, the wind speed cubed at a five year lag was the most important predictor variable. He hypothesized that a deeper mixed layer provides favorable foraging habitat for juvenile albacore, which in turn results in faster growth, and greater spawning and recruitment in later years, perhaps explaining the lagged correlations. Although remote sensing revealed that the CCS encompasses areas with high frontal activity and several studies have documented the relationship of albacore with fronts, there are few quantitative studies of this relationship overall, and none in the Northeast Pacific. Previous studies were based on shorter time series and/or coarser spatial resolution. In this study, we used SST imagery to detect mesoscale fronts and boosted regression tree (BRT) models to quantify the relationship between these frontal features and other environmental variables like SST and chlorophyll to albacore distribution in the coastal waters of the Northeast Pacific over 24 years.

2. Methods

2.1. Albacore CPUE data

The study area was located in the Northeast Pacific (30–55° N), from the coast to 200 nm offshore (370km, coastal region, black line on Figure 1). Albacore catch and effort data were assembled from vessel logbooks of U.S. (1961-2011) and Canadian (2004-2011) albacore troll and pole-and-line vessels, using databases managed by the U.S. National Marine Fisheries Service and the Department of Fisheries and Ocean Canada. The US and Canadian CPUE abundance indices were compared and found to be similar (*Teo et al.*, 2010a) and the US-Canadian merged index has been used in this analysis. The assembled data contained albacore catch (numbers of albacore caught) and effort (number of vessel fishing days), as well as the date (year, month and day) and location (latitude and longitude with resolution in minutes) of fishing. Although the albacore logbook data are available from 1961, preliminary inspection of the data showed that prior to 1988, there was negligible amount of logbook data with fine-scale location information ($< 1°$) necessary to relate albacore distribution to fine-scale frontal features. Therefore, only data from 1988-2011 were used in the BRT models. We aggregated the albacore catch and effort data into 0.25° resolution spatial grids at monthly intervals in order to reduce the noise in the data and simplify the problem. This resulted in a total of 22,448 aggregated CPUE (number of albacore caught per vessel day) observations in our study area, with the largest number of CPUE strata in the coastal area off Washington and Oregon (Figure 1).

2.2. Satellite data

Sea surface temperatures were computed from Advanced Very High Resolution Radiometer (AVHRR) Pathfinder Version 5.2 daily data with nominal 4 km resolution (ftp://ftp.nodc.noaa.gov/pub/data.nodc/pathfinder/Version5.2/). We processed a total of 10,532 daily images for the period 1982–2011. Sea-surface chlorophyll concentration was estimated from daily, level 2, 4-km resolution Sea-Viewing Wide-Field (SeaWiFS) and Moderate Resolution Imaging Spectroradiometer (MODIS) for the period 1998–2002 and 2003–2011 respectively. (http://oceancolor.gsfc.nasa.gov/). The geostrophic current data were produced by Ssalto/Duacs distributed by Archiving, Validation, and Interpretation

of Satellite Oceanographic (AVISO)(http://www.aviso.oceanobs.com/duacs/), with support from CNES. We used the meridional and zonal weekly geostrophic current component products at 0.25° resolution computed by AVISO from the sea level anomalies.

2.3. Fronts detections and gradients

We used an improved version of the Cayula-Cornillon algorithm adapted for upwelling systems to detect fronts in SST imagery (*Nieto et al.*, 2012). The advantage of this approach, compared to the gradient-based methods which generate a continuous field of values, is that only the edges are retained between two water masses, which allowed us to accurately compute the distance of fishing locations to the nearest front, as well as to calculate the temperature gradient across the front. Positive distances indicate fishing locations were offshore of the nearest fronts (negative: inshore). If the distance from the fishing location to the coast is less than the distance of the nearest front from the coast, we assigned a negative value for this distance, and vice versa. We used the frontal index described by *Nieto et al.* (2012) to create frontal-intensity maps from a combination of front edge images and front gradient images. We used the Sobel edge enhancement kernel to calculate front gradient images. The gradient value was extracted and assigned to the front edge, on a pixel by pixel basis, to compose frontal gradients. To synthesize the results of the frontal gradient images in space and time, we created an average frontal index over all times. We also computed the average value of the frontal index by latitude from the coast to 200 nm. The perimeter of the area with mean spring-time albacore CPUE higher than the 50th percentile was overlaid on the mean spatial pattern of the 1982–2011 frontal index.

2.4. Modeling

We applied a BRT analysis to model the albacore CPUE distribution in relation to frontal features and other environmental variables. The BRT was performed using the "gbm" package (version 2.0-8) in R (version 2.15.1, R Developmental Core Team, 2012) with the following settings: 1) Gaussian family; 2) moderate number of nodes in a single tree (tree complexity = 3); 3) moderate contribution from each tree (learning rate = 0.05); and 4) moderate levels of stochasticity (bag fraction = 0.5), which resulted in a good balance between model complexity and computation speed. We tested the settings in preliminary models and found that the results were not sensitive to the settings that were chosen. We filled with missing values the chlorophyll and geostrophic current time series prior to1998 and 1992 respectively to match the length of the CPUE and SST time series. Filling with missing values did not affect the results because the BRT model handles missing values properly by introducing surrogate splits. The CPUE response variable was log-transformed [log(CPUE+0.001)] prior to analysis because the CPUE data had a lognormal distribution. We first examined a preliminary BRT model using all environmental variables in Table 1 plus month and year as predictor variables. Predictor variables were not included in the final BRT model if they were highly correlated (Pearson's $r > 0.5$) or were small contributors ($< 5\%$) to the explanatory power of the model. We found that SST at fishing locations (SST) was highly correlated (r = 0.93, Table 2) with SST at fronts (SST_{FRONT}). Distance from the fishing location to the coast (D_{COAST}) was also highly correlated (r = 0.99, Table 2) with distance between fronts and the coast ($D_{FRONT-COAST}$) because the vast majority (95%) of fishing activities occurred within 5 km of the fronts. Based on these correlations, SST_{FRONT} and D_{COAST} were not used as predictor variables in the the final BRT model. We also noticed that SST gradients at fishing locations ($GRAD$) and gradients at the fronts ($GRAD_{FRONT}$) were small contributors in the preliminary model (4.0% and 1.3% respectively, Appendix 1), and so they were excluded from the final model. With these considerations, we retained six environmental variables and two temporal factors (year and month), and re-fit the BRT model. To test the robustness of the final BRT model, we used leave-one-year-out cross-validation. For each year in turn, data from that specific year were used as the testing set and excluded from the other 23 years of data used as the training set. We examined model performance (i.e., variance explained) at each cross validation step, and compared the observed and model-predicted CPUE by calculating the root mean square error of the model for each year.

3. Results

3.1. Predicting albacore CPUE

Including all variables in Table 1 plus month and year, the preliminary BRT explained about 33.3% of the total variance. Using only eight explanatory variables (four less than the preliminary model), the final BRT model explained

slightly less (31.7%) of the total variance than the preliminary model. Differences between the preliminary and final models and relative contribution of different variables are showed in Appendix 2. The SST at fishing locations was the largest contributor (relative contribution = 19.1%), followed by chlorophyll concentration (16.6%) and distance of the front from the coast (16.3%). Seasonal and interannual changes contributed 12.0% and 11.5%, respectively (Figure 2).

There was a positive relationship between log_{CPUE} and SST, and a negative relationship between log_{CPUE} and *chlorophyll*, which suggested albacore CPUE is higher in warmer, low-chlorophyll waters (Figure 2). Albacore CPUE was also higher near the fronts (Figure 2), with mean CPUE at approximately 80 albacore per boat days within 50 km of the front, and less than half of that elsewhere (Figure 3). Albacore fishermen clearly make use of this relationship by fishing close to the fronts, with 95% of the effort being distributed within 0–5 km of the fronts (Figure 3). Albacore abundance along the Northeast Pacific coast varied seasonally and interannually, being most abundant during summer (July, August and September) and with higher abundance after 2000 with the exception of low catches in 2005 and 2011 (Figure 2).

The BRT model was able to successfully represent the observed spatial patterns of albacore CPUE but was unable to explain some of the very high observed CPUEs in some areas. Here we provide an example of predicted and observed CPUE in August 2010-2011 (Figure 4). The spatial distribution of SST, chlorophyll, frontal gradients and geostrophic current vectors in August 2010 and 2011 are shown in Figure 4a, b, c, d and Figure 4g, h, i, j respectively. Observed and model-predicted CPUEs for both August 2010 and 2011 show higher CPUEs inshore of about 100km from the coast, concentrated in warmer, low chlorophyll water off Oregon, Washington and Vancouver Island (Figure 4e, f and Figure 4k, l respectively). Although the model was able to reproduce the observed spatial and temporal patterns of albacore CPUE, the observed CPUE was more variable than predicted (Figure 4e,k , Table 4).

Cross-validation showed that BRT model performance was robust through time. Overall variance explained by the BRT models was relatively similar (31.7 ± 1.1%) over 24 years. The relative contribution of predictor variables to the total explained variance of the BRT models remained relatively similar through time, with low standard deviations relative to the mean contributions (Table 3). For training sets, the predicted mean log_{CPUE} was very similar to observed mean log_{CPUE}, and the standard deviations were about half of the observed log_{CPUE}. Similar averaged mean and standard deviations were found for the testing sets. Root mean square errors were more variable for training sets at the beginning of the time series but were comparable after 1999 (Table 4). This was likely due to small sample sizes because submission of vessel logbooks were not mandatory during the early period and albacore vessels fished more in coastal waters after 1999 (Appendix 3).

3.2. Spatio–temporal patterns of fronts in the central and northern CCS

Most of the higher CPUE data are concentrated between 40° and 50° N (Figure 5). North of Cape Blanco (~ 43°N), higher CPUE are located just beyond the frontal area, with fronts aligned parallel to the coast (in contrast to filaments, which are fronts aligned approximately normal to the coast (*Nieto et al.*, 2012)). However, between Cape Mendocino (around 40° N) and Cape Blanco, higher CPUE are found in the frontal area. This area, unlike the area north of Cape Blanco, is characterized by filaments.

The frontal index was highest during May–June between Point Arenas (~ 38°) and Cape Mendocino (~ 40°N), and from Cape Blanco (~ 43°N) to 45° (Figure 5). The alignment of the coastline in this region is predominately north-south compared to south of Point Arena and the fronts show some indication of association with capes. South of Point Arena (~ 38°) the frontal zone extends far offshore, but the fronts are more dispersed and there are more filaments. Fronts decrease north of 45° N, with the exception in the area around the Strait of Juan Fuca (~48°N) at the end of the summer season and beginning of fall season (Figure 5).

Hovmöller plots show the relationships between the front index, distance of the fronts from the coast, SST and chlorophyll through space and time (Figure 6). Frontal activity is highest in summer and early fall (August, September and October, Figure 6a). Distance of the fronts from the coast differs with latitude. At 33–34°N, fronts are further offshore (>160 km), compared to ~52°N where fronts are closer to shore (<100 km) than anywhere else in the study area (Figure 6b). As is well known, seasonality reflected in SST is stronger in the northern part of our study area (Figure 6c). As seasonal wind-driven upwelling develops, the contrast between cool coastal water and warmer water further offshore produces stronger fronts along the central California coast, between 36–43°N or approximately between Monterey and Cape Blanco (Figure 6a). It is noteworthy that greater frontal activity in the summer (Figure

6a) is not associated with higher chlorophyll (Figure 6d). Chlorophyll is higher north of ~45°N, in the spring and summer seasons, and low in the areas with strongest frontal activity (Figure 6d).

4. Discussion

Previous studies have shown that albacore tuna habitat is found primarily in waters with SSTs between 12–22°C. For example, juvenile albacore, after migrating to the North American west coast in the summer, were more abundant in 15–19.5° C water (*Clemens*, 1961; *Flittner*, 1963; *Laurs et al.*, 1977). Using archival tag data, *Childers et al.* (2011) found albacore in temperatures ranging from 11.9–22.3°C (mean = 17.6°C). *Pearcy* (1970) indicated that albacore avoided warm Columbia River plume water, but were found in temperatures of approximately 15.5°C, in proximity to strong horizontal SST gradients. Avoidance of the river plume may have more to do with the low salinity lens associated with the river outflow than with temperature. Our study also found that temperature is the most important environmental variable for predicting albacore CPUE. Higher albacore CPUE was associated with SST higher than 18°C. Albacore may try to stay in warm water to maintain body temperature and minimize heat loss (*Collette*, 1978; *Phillips*, 2011; *Phillips et al.*, 2014). Like other tunas, the response of albacore CPUE to SST is likely to be dome-shaped with a peak higher than 18°C (*Teo and Block*, 2010b) but Northeast Pacifc coastal areas are relatively cool and albacore there are not likely to experience SSTs that warm in this region (see Figure 6c).

Barth et al. (2000) suggested that Cape Blanco (~ 43° N) is a dividing point between a region to the north where upwelling is fairly well confined to the continental shelf and an area south of Cape Blanco where a meandering equatorward jet and upwelled water extend well seaward of the continental margin. Persistent sites of filament generation in the central CCS are Cape Mendocino (~ 40° N) and Point Arena (~ 38° N) (*Randerson and Simpson*, 1993). We also found high frontal activity between Cape Mendocino and Point Arena, and we observed an area of energetic fronts and filaments in the vicinity of Cape Blanco. *Strub et al.* (1991) pointed out that filaments and currents meander in this area and can extend several hundred kilometers from the coast.

The high values of chlorophyll are usually found in the coastal area associated with upwelling waters. The area beyond the frontal system (and beyond the upwelling area), where the albacore are mainly distributed (Figure 5) is associated with areas of lower chlorophyll. Within the area beyond the frontal system, the albacore will be close to the fronts where the availability of food will be relatively higher. If we assume that distance from front to the coast ($D_{FRONT-COAST}$) is directly associated to upwelling and that CPUE is distributed mainly near the fronts, we could infer the albacore distribution will be near or far to the coast depending of the position of the upwelling fronts.

Similar to previous work, our study confirmed that albacore fishing activity is closely associated with frontal features. Highest mean albacore CPUE occurred within about 75 km of fronts and dropped substantially at greater distance from the fronts. Albacore fishermen clearly use frontal features to guide their fishing activities since the vast majority of fishing effort occured within 5 km of the fronts. Interestingly, fishing activities were more concentrated on frontal features (within 5 km) than is necessitated by the decline in albacore CPUE relative to the fronts. *Laurs et al.* (1984) suggested that albacore stay on the warm and less productive side of fronts. By using higher resolution data, we found that the situation is more complex due to the structure of fronts. Whether higher albacore CPUEs are on the warm or cool side of fronts depends on which front the CPUE are referenced to, because there are many discrete SST fronts constituting the frontal zone that we studied. If referring to the major upwelling front near the coast, then major fishing activities were on the warmer side (Figure 5). However, as we have shown, the actual distribution is more complex than the averaged spatial field of fronts because the averaging smooths out the spatial complexity of many discrete SST fronts. The complexity of the frontal system, visible in the daily, weekly and even in the monthly images that we used in this study makes it a difficult task to classify a fishing location as being on one or the other side of fronts and can lead to misinterpretation. What may be the warm side of one front can be the cold side of another nearby front located a little farther from the coast.

As discussed by *Nieto et al.* (2012) the front detection method used in this study is particularly useful in spatially complex frontal regions associated with coastal upwelling. Our results show that the frontal system in this region is made up from a complex set of fronts and filaments originating from upwelling activity and likely molded by the presence of capes and other physical characteristics. Even if we are able to infer the presence of filaments from the imagery, to include this variable in the BRT model we would need classify the filaments in a quantitative way. Since we have already identified the fronts in this area, in the future we could implement the method proposed by *Nieto et al.* (2012) to determine which of these fronts could be classified as filaments. The importance of the filaments resides

in the subduction processes associated with them (in contrast to the convergent processes associated with fronts). Subduction may transport prey out of the nutrient rich filament and into offshore oceanic waters. As pointed out by *Randerson and Simpson* (1993), albacore habitat is found in oligotrophic offshore waters. This may be possible in part because mesoscale filaments could transport prey to offshore oceanic areas, providing localized prey concentrations to otherwise oligotrophic waters.

The BRT model showed that the contribution of geostrophic currents was small and that albacore were associated with absolute current velocities near zero. This finding contrasts with reports from other studies (Zainuddin et al., 2008; Goikoetxea et al., 2014) that albacore are positively related to geostrophic currents, perhaps because the fish were associated with eddy edges in these studies. However, our study focused on the coastal area and it may be that the relationships between eddies, currents and albacore distribution differ between the open ocean and coastal areas. A finer scale study would be useful to resolve these relationships.

Our study relied on fisheries data, which have several limitations when used for scientific purposes. First, the unit of effort used in the CPUE calculation (vessel-days) is a crude measure of effort and may not account for differences in fishing power among vessels nor changes in day length as the season progresses (fishing operations only occur during day light hours and the fishing season is approximately mid-June to the end of October), which may produce more noise in the results as a consequence. Other metrics of effort for the CPUE calculation that could address these limitations, such as jig-hours (number of jigs (lines) fished x number of hours fished), are not available for both the Canadian and United States albacore fleets. Second, commercial fisheries data are subject to changes in catchability (number of fish or biomass per unit of effort) over time, which can affect estimates of CPUE. Changes in catchability are important when CPUE is used as a measure of relative stock abundance, but in our study the spatial distribution of CPUE is important rather than whether CPUE changes through time. Changes in catchability should not affect the spatial distribution of CPUE. Third, the spatial distribution of CPUE depends on daily positions recorded by fishermen. There is uncertainty in these positions because we do not know when during the fishing operation (beginning, middle, end) the position is taken and recorded in a log book. We assumed in our study that the uncertainty in fishing locations is constant over time, i.e., the magnitude of uncertainty does not change between years. Fourth, fishermen have adopted technology which enhances their ability to find albacore based on SST temperatures. *Laurs et al.* (1984) pointed out that albacore fishermen on the west coast of North America used SST data and ocean colour boundary charts in the 1980s and probably adopted SST maps once they became widely available. Many vessels in this fleet are equipped with SST sensors and fishermen use visual cues to detect and fish along SST fronts. Despite these advantages, catches along fronts are variable and we were interested in assessing whether distance to the front or the magnitude of the front explains or contributes to an explanation for this variability in catches.

This paper is a first step toward a more comprehensive quantitative assessment of environmental effects on albacore distribution in the northeast Pacific Ocean. The next step is to use these results to improve abundance indices derived from the same datasets, which will in turn improve our assessment of this stock. In a previous paper (*Xu et al.*, 2013), we showed that the CPUE indices derived from the US-Canada albacore troll and pole-and-line fisheries are largely driven by data from the coastal region. This suggests that we may be able to identify the key coastal environmental effects and derive better standardized CPUE indices for future stock assessments. In addition, there is substantial interest in understanding and predicting potential changes in albacore distribution in the Northeast Pacific with changing environmental conditions, especially in the face of climate change. Albacore tuna in the coastal CCS straddles the U.S.-Canadian border and the effort of the US fleet in Canadian waters (and vice versa) is managed by the US-Canada albacore treaty, which is renegotiated at regular intervals. Therefore, as the albacore distribution shifts north-south or offshore-onshore, the availability of albacore to these coastal fisheries likely changes. Fishermen have been using SST imagery to make fishing decisions for a long time. The techniques applied in this paper could be used to create near real-time probability maps of albacore distribution based on current environmental conditions, which may substantially benefit fishers and fisheries management, including U.S.-Canada treaty negotiations, in a timely manner.

Acknowledgements

The authors acknowledge all US and Canadian fishermen who reported the albacore catch data in logbooks. We thank two internal reviewers Dr. Toby Garfield and Dr. Paul Fiedler for their suggestions and comments. This research was supported by the NOAA-FATE program.

References

Barth, J.A., Pierce, S.D., and R.L. Smith (2000), A separating coastal upwelling jet at Cape Blanco, Oregon and its connection to the California Current System,textitDeep Sea Research Part II: Topical Studies in Oceanography, *47*(5), 783–810. doi: 10.1016/S0967-0645(99)00127-7

P. A. Bernal (1979), Large-scale biological events in the California Current, *Calif.Coop.Oceanic Fish.Inv.Rep*, *20*, 89–101

S. B. Brandt (1993), The Effect of Thermal Fronts on Fish Growth: A Bioenergetics Evaluation of Food and Temperature , *Estuaries*, *16*(1), 142–159.

Brodeur, R.D., E. Howell, J. Polovina, L. Ciannelli, W.G. Pearcy, R.M. Laurs, and J. Childers (*unpublished manuscript*), Spatial and temporal variations in albacore habitat in the northeast Pacific using remotely-sensed environmental data.

Childers, J., Snyder, S. and S. Kohin (2011), Migration and behavior of juvenile NorthPacific albacore (*Thunnus alalunga*), *Fisheries Oceanography*, *20*, 157–173. doi: 10.1111/j.1365-2419.2011.00575.x.

H. B. Clemens (1961), The migration, age, and growth of Pacific albacore (*Thunnus germo*), 1951-1958, *California Department of Fish and Game, Fish Bulletin*, *115:128*

B. B. Collette (1978), Activity of albacore serum complement reflects its thermoregulatory capacity, *In The physiological ecology of tunas (G.D. Sharp and A.E. Dizon, eds.)*, *Academic Press Inc.*,7–39

Fiedler, P., and H. Bernard (1987), Tuna aggregation and feeding near fronts observed in satellite imagery, *Continental Shelf Research*, *7*(8), 871–881.

G. A. Flittner (1963), Review of the 1962 seasonal movement of albacore tuna off the Pacific coast of the United States, *Commercial Fisheries Review*, *25*(4), 7–13.

Lan, H., Kawamura, H., Lee, M.–A., Lu H.–J., Shimada, T., Hosoda, K., and F. Sakaida (2012), Relationship between albacore (*Thunnus alalunga*) fishing grounds in the Indian Ocean and the thermal environment revealed by cloud-free microwave sea surface temperature, *Fisheries Research*, *113*(1), 1–7.

Laurs, R.M. and R.J. Lynn (1977), Seasonal migration of North Pacfic albacore, *Thunnus alalunga*, into North American coastal waters: Distribution, relative abundance, and association with transition zone waters, *Fisheries Bulletin*, *75*, 795.

Goikoetxea, N., Fontan, A., Caballero, A., Santiago, J., Goni, N., Arrizabalaga, H., Sagarminaga, Y., Chifflet, M., Arregi, I., and J. Mader (2014), Influence of oceano-meteorological conditions on the behaviour, distribution and abundance of the northeast Atlantic albacore, *Collect. Vol. Sci. Pap. ICCAT*,*70*(3), 1256–1275.

Laurs, R.M., Fielder, P.C. and D.R. Montgomery (1984), Albacore tuna catch distributions relative to environmental features observed from satellites., *Deep-Sea Research*,*31*, 1085–1099.

Nieto, K., H. Demarcq, and S. McClatchie (2012), Mesoscale frontal structures in the Canary Upwelling System: New front and filament detection algorithms applied to spatial and temporal patterns, *Remote Sensing of Environment*, *123*, 339–346, doi10.1016/j.rse.2012.03.028.

W. G. Pearcy (1970), Albacore oceanography off Oregon-1970, *Fishery Bulletin*, *71*(2), 489–504.

A. J. Phillips (2011), Long Term Albacore (*Thunnus alalunga*) Spatio-temporal Association with Environmental Variability in the Northeastern Pacific, *MS Thesis. Oregon State University.*, *140 pp.*

Phillips, A. J., Ciannelli, L., Brodeur, R. D., Pearcy, W. G., and Childers (2014), Spatio–temporal associations of albacore CPUEs in the Northeastern Pacific with regional SST and climate environmental variables,textitICES Journal of Marine Science, *71*(2), doi.10.1093/icesjms/fst238

Polovina, J., Howell, E., Kobayashi, D.–R., and M.–P. Seki (2001), The transition zone chlorophyll front, a dynamic global feature defining migration and forage habitat for marine resources, *Progress in Oceanography*, *49*(1–4), 469–483.

Randerson, J.T., and J.J. Simpson (1993), Recurrent patterns in surface thermal fronts associated with cold filaments along the West Coast of North America, *Remote Sensing of Environment*, *46*(2), 146–163.

Strub, P.T., Kosro, P.M., and A. Huyer (1991), The nature of the cold filaments in the California Current system,textitJournal of Geophysical Research, *96*(C8), 14743–14768.

Teo, S.L.H., Holmes, J. and S. Kohin (2010a), Joint standardized abundance index of US and Canada albacore troll fisheries in the North Pacific, *ISC/10-3/ALBWG/01*

Teo, S.L.H., and B.A. Block (2010b), Comparative Influence of Ocean Conditions on Yellowfin and Atlantic Bluefin Tuna Catch from Longlines in the Gulf of Mexico, *PLoS ONE*, *5*(5),e10756. doi:10.1371/journal.pone.0010756

Thomas, A.C., and P.T. Strub (2001), Cross-shelf phytoplankton pigment variability in the California Current, *Continental Shelf Research*, *21*, 1157–1190.

Xu, Y., Teo, S. and J. Holmes (2013), An update of the standardized abundance index of US and Canada albacore troll fisheries in the North Pacific (1966-2012), *ISC/13/ALBWG-03/06*, $isc.ac.affrc.go.jp/pdf/ALB/ISC13_ALB_2/ISC_13_ALBWG_0306_Xu_v3.pdf$.

Zainuddin, M.,, Kiyofuji, H., Saitoh, K., and S.–I. Saitoh (2006), Using multi-sensor satellite remote sensing and catch data to detect ocean hot spots for albacore (*Thunnus alalunga*) in the northwestern North Pacific,textitDeep Sea Research Part II: Topical Studies in Oceanography, *53*(3–4), 419–431.

Zainuddin, M., Saitoh, K., and S.–I. Saitoh (2008), Albacore (*Thunnus alalunga*) fishing ground in relation to oceanographic conditions in the western North Pacific Ocean using remotely sensed satellite data,textitFisheries Oceanography, *17*(2), 61–73.

Table 1. The units, mean, range and description of environmental variables used in the BRT model.

Variables	Units	Mean	Range	Description	Retained in final BRT model
chlorophyll	mg/m^3	0.74	0.026–22.73	chlorophyll concentration at the fishing location	Yes
SST_{FRONT}	$^{\circ}C$	15.16	8.78–19.49	Sea surface temperature at the nearest front	No
SST	$^{\circ}C$	15.21	8.79–19.51	Sea surface temperature at the fishing location	Yes
gc_V	m/s	-0.0362	-0.36–0.30	Meridional geostrophic current at the fishing location	Yes
gc_U	m/s	-0.0011	-0.41–0.39	Zonal geostrophic current at the fishing location	Yes
D_{FRONT}	km	0.3	-179.33–181.98	Distance from the fishing location to the front	Yes
D_{COAST}	km	151.48	3.84–413.09	Distance from the fishing location to the coast	No
$D_{FRONT-COAST}$	km	150.15	5.97–414.95	Distance from the front to the coast	Yes
$GRAD$	$^{\circ}C/km$	0.044	0–0.29	SST gradient at the fishing location	No
$GRAD_{FRONT}$	$^{\circ}C/km$	0.0079	0–0.392	SST gradient at the nearest front	No

Table 2. Correlation matrix table between D_{FRONT}, D_{COAST},$D_{FRONT-COAST}$,GRAD_{FRONT},$GRAD$, SST, SST_{FRONT},gc_U, gc_V, and *chlorophyll*. Environmental variables with correlation coefficients >0.5 (*) were excluded from the final model. Pearson's r values are in the upper triangle and p-values are in the lower triangle.

	D_{FRONT}	D_{COAST}	$D_{FRONT-COAST}$	$GRAD_{FRONT}$	$GRAD$	SST	SST_{FRONT}	gc_U	gc_V	*chlorophyll*
D_{FRONT}		0.05	0.05	-0.03	-0.07	0.02	-0.02	0.01	0.01	-0.05
D_{COAST}	<0.0001		0.99*	-0.13	-0.25	0.28	0.27	0.04	0.01	-0.42
$D_{FRONT-COAST}$	<0.0001	<0.0001		-0.13	-0.25	0.28	0.27	0.04	0.00	-0.42
$GRAD_{FRONT}$	<0.0001	<0.0001	<0.0001		0.37	-0.09	-0.07	-0.01	-0.03	0.15
$GRAD$	<0.0001	<0.0001	<0.0001	<0.0001		0.14	-0.12	-0.05	-0.02	0.22
SST	<0.0001	<0.0001	<0.0001	<0.0001	<0.0001		0.93*	0.06	-0.09	-0.25
SST_{FRONT}	<0.0001	<0.0001	<0.0001	<0.0001	<0.0001	<0.0001		0.06	-0.09	-0.24
gc_U	0.0042	<0.0001	<0.0001	0.36971	<0.0001	<0.0001	<0.0001		-0.10	-0.11
gc_V	<0.0001	<0.0001	<0.0001	<0.0001	<0.0001	<0.0001	<0.0001	<0.0001		0.00
chlorophyll	<0.0005	<0.0001	<0.0001	<0.0001	<0.0001	<0.0001	<0.0001	<0.0001	<0.0001	

Table 3. Mean, standard deviation and coefficient of variation for total explained variance and relative contribution of all variables in the final boosted regression tree model. Mean and SD are calculated using the leave-one-year-out analysis (N=24)

Variables	Mean ± SD %	Coefficient of Variation
Total explained variance	31.74 ± 1.12	0.035
SST	18.77 ± 0.73	0.039
chlorophyll	17.05 ± 0.65	0.038
$D_{FRONT-COAST}$	16.12 ± 0.65	0.040
month	11.95 ± 0.72	0.060
year	11.64 ± 0.97	0.083
D_{FRONT}	9.18 ± 0.74	0.081
gc_U	6.15 ± 0.57	0.093
gc_V	9.13 ± 0.64	0.070

Table 4. Cross-validation of predicted log_{CPUE}, observed log_{CPUE} and root mean square error for training set and testing set over 24 years.

Year Left Out	Training Set			Testing Set		
	Observed log_{CPUE} Mean±SD	Predicted log_{CPUE} Mean±SD	Root Mean Square Error	Observed log_{CPUE} Mean±SD	Predicted log_{CPUE} Mean±SD	Root Mean Square Error
1988	3.33 ± 2.66	3.33 ± 1.32	2.15	2.99 ± 3.46	1.73 ± 1.30	3.42
1989	3.36 ± 2.64	3.36 ± 1.32	2.13	1.29 ± 3.88	0.05 ± 2.59	4.70
1990	3.36 ± 2.63	3.36 ± 1.29	2.14	1.72 ± 3.92	2.10 ± 1.50	3.73
1991	3.34 ± 2.66	3.35 ± 1.28	2.18	2.07 ± 3.41	2.53 ± 1.71	3.20
1992	3.34 ± 2.65	3.34 ± 1.24	2.21	2.78 ± 3.55	1.93 ± 1.28	3.39
1993	3.33 ± 2.69	3.33 ± 1.32	2.19	2.97 ± 2.32	2.21 ± 1.27	2.41
1994	3.34 ± 2.66	3.35 ± 1.31	2.16	2.70 ± 3.35	2.52 ± 1.13	3.31
1995	3.36 ± 2.65	3.36 ± 1.31	2.15	1.85 ± 3.30	2.77 ± 1.06	3.39
1996	3.34 ± 2.67	3.34 ± 1.30	2.18	2.61 ± 3.16	2.41 ± 1.15	3.12
1997	3.35 ± 2.67	3.35 ± 1.32	2.16	2.48 ± 2.92	1.60 ± 1.39	3.10
1998	3.32 ± 2.68	3.33 ± 1.28	2.22	3.34 ± 2.81	3.22 ± 1.08	2.57
1999	3.35 ± 2.69	3.35 ± 1.31	2.20	2.87 ± 2.42	3.24 ± 1.24	2.28
2000	3.33 ± 2.69	3.33 ± 1.29	2.21	3.25 ± 2.45	3.65 ± 1.26	2.26
2001	3.31 ± 2.70	3.31 ± 1.30	2.22	3.61 ± 2.09	3.27 ± 1.34	2.24
2002	3.31 ± 2.68	3.31 ± 1.30	2.19	3.59 ± 2.74	3.76 ± 1.01	2.52
2003	3.30 ± 2.69	3.31 ± 1.29	2.22	4.05 ± 2.05	3.86 ± 0.85	1.87
2004	3.26 ± 2.72	3.26 ± 1.29	2.25	4.26 ± 1.77	3.73 ± 0.91	1.73
2005	3.32 ± 2.71	3.32 ± 1.34	2.20	3.34 ± 2.36	4.00 ± 0.85	2.31
2006	3.26 ± 2.72	3.26 ± 1.32	2.23	4.22 ± 1.79	3.70 ± 0.94	1.81
2007	3.28 ± 2.71	3.29 ± 1.34	2.19	3.84 ± 2.14	3.61 ± 1.19	2.14
2008	3.32 ± 2.65	3.32 ± 1.31	2.15	3.33 ± 3.06	3.69 ± 0.99	2.79
2009	3.29 ± 2.70	3.29 ± 1.35	2.18	3.82 ± 2.29	3.48 ± 1.23	2.21
2010	3.30 ± 2.71	3.31 ± 1.34	2.22	3.56 ± 2.22	3.14 ± 1.18	2.23
2011	3.34 ± 2.69	3.34 ± 1.35	2.16	3.15 ± 2.59	3.66 ± 0.98	2.47
Average	3.32 ± 2.68	3.33 ± 1.31	2.19	3.07 ± 2.75	2.91 ± 1.23	2.72

5. Figure captions

Figure 1: Study region and numbers of CPUE observations at 0.25° spatial resolution. Strata with ≤ 3 vessels are not shown due to data confidentiality. Black line is the 200 nautical miles isoline.

Figure 2: Boosted regression tree fitted function of 8 predictors and summary of relative contributions (31.7% total explained variance). Black dots are 100 values generated by BRT model to describe the fitted function. Red lines are polynomial fit curves of the dots.

Figure 3: A) Catch-per-unit-effort (fish/boat day, red circles) and number of CPUE observations (open black bars) with respect to distance to nearest front (N=22,448). B) The mean, median, quantile-25% and quantile-75% CPUE at different distance to the nearest front.

Figure 4: Comparison of predicted (b, h) and observed CPUE (a, g) for 2010 and 2011, associated with SST (c, i), chlorophyll (d, j), front gradient (e, k) and geostrophic currents (f, l). Black line is the 200 nautical miles isoline.

Figure 5: Average image of front index (1982–2011 period). Black polygon shows the area where the CPUE was greater than the average during the spring season.

Figure 6: Hovmöller diagrams of monthly climatology of front index, front distance, SST and chlorophyll (average from coast to 200 nm)

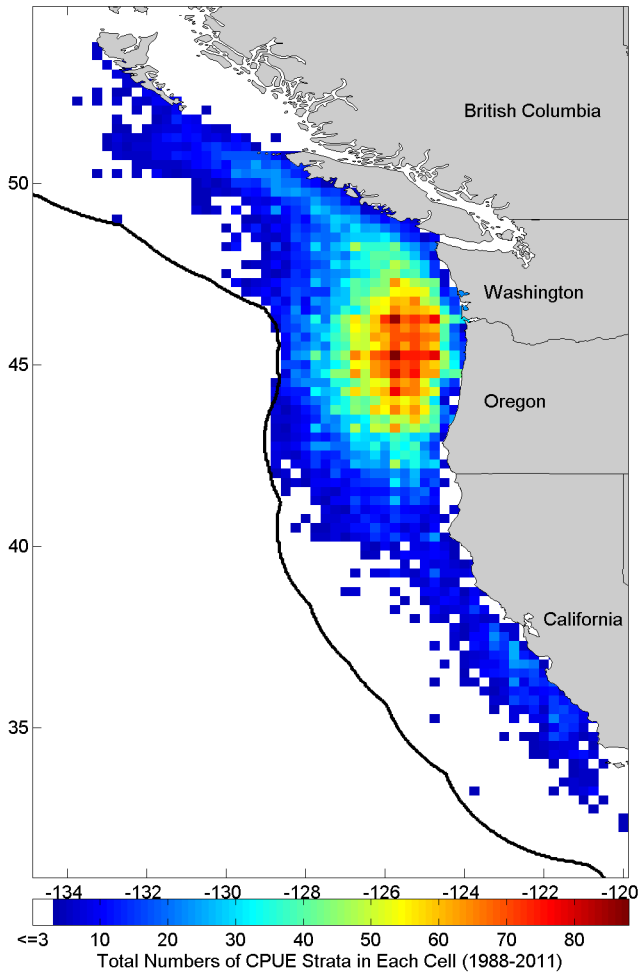
British Columbia
Washington
Oregon
California
50
45
40
35
-134
-132
-130
-128
-126
-124
-122
-120
<=3
10
20
30
40
50
60
70
80
Total Numbers of CPUE Strata in Each Cell (1988-2011)

Figure 1.

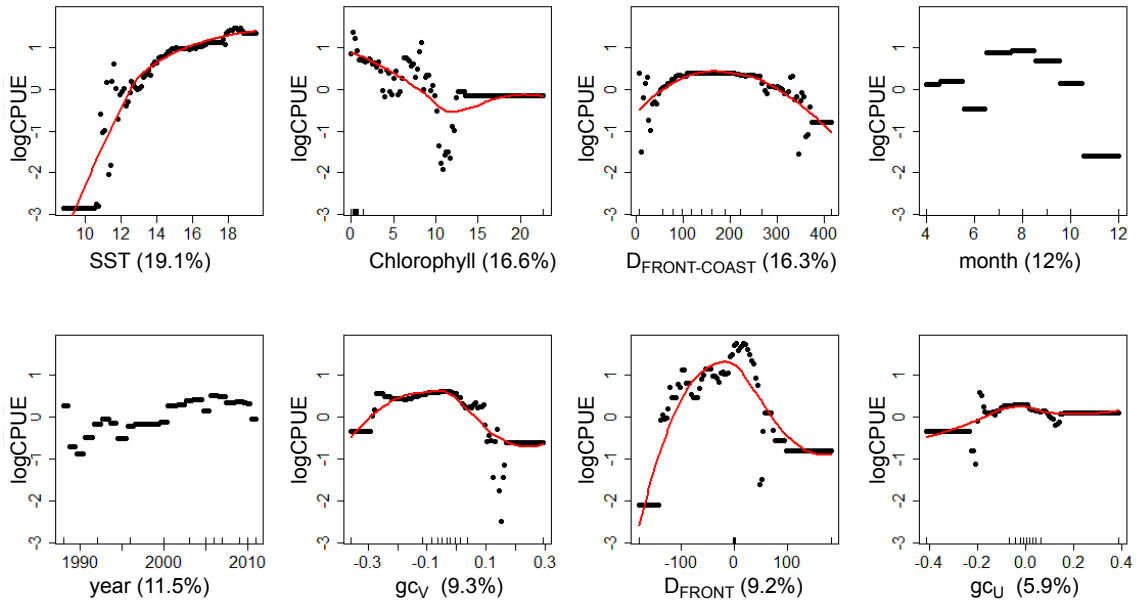
logCPUE
SST (19.1%)
Chlorophyll (16.6%)
$D_{FRONT-COAST}$ (16.3%)
month (12%)
year (11.5%)
gc_V (9.3%)
D_{FRONT} (9.2%)
gc_U (5.9%)

Figure 2.

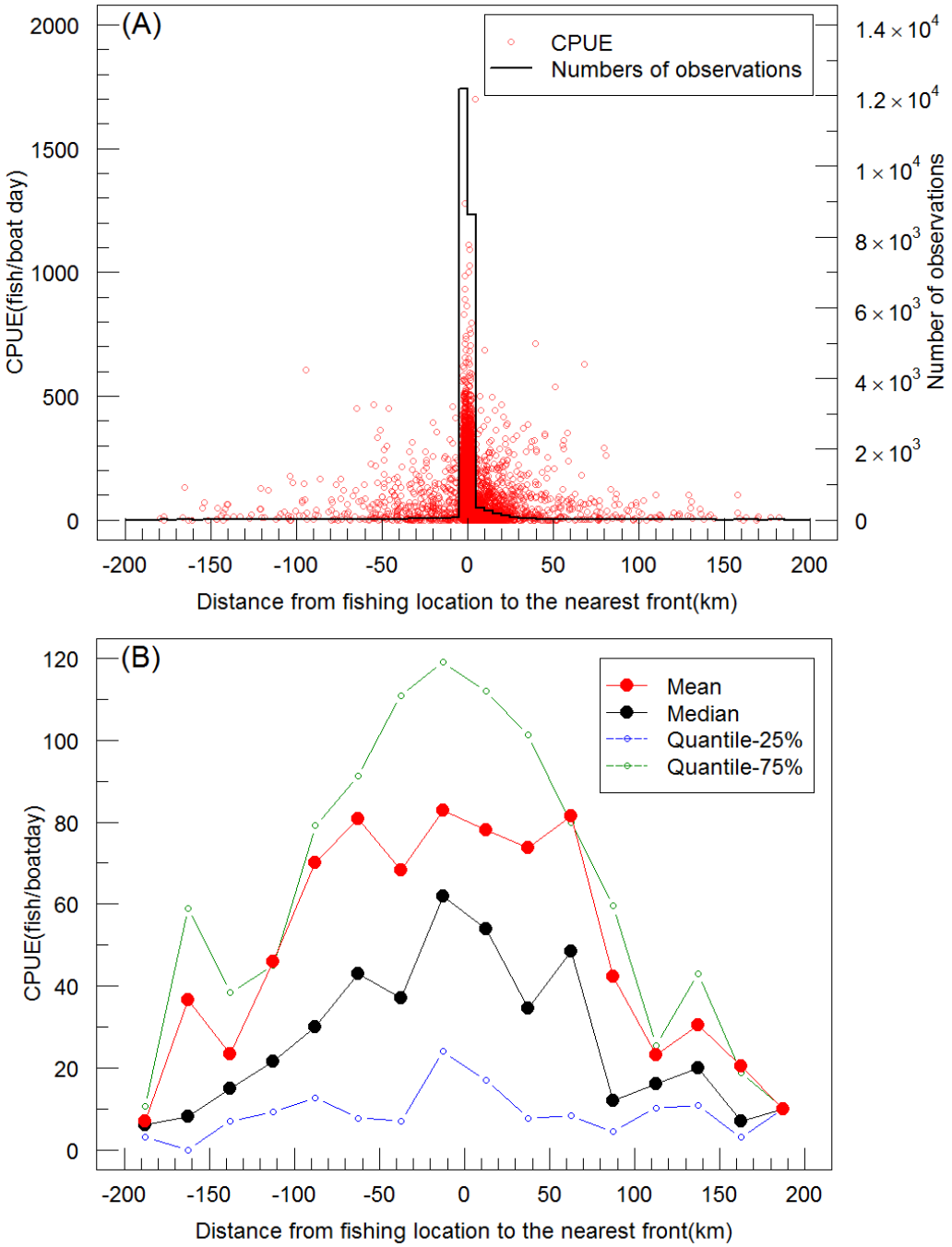
(A)
CPUE
Numbers of observations
CPUE(fish/boat day)
Number of observations
Distance from fishing location to the nearest front(km)
(B)
Mean
Median
Quantile-25%
Quantile-75%
CPUE(fish/boatday)
Distance from fishing location to the nearest front(km)

Figure 3.

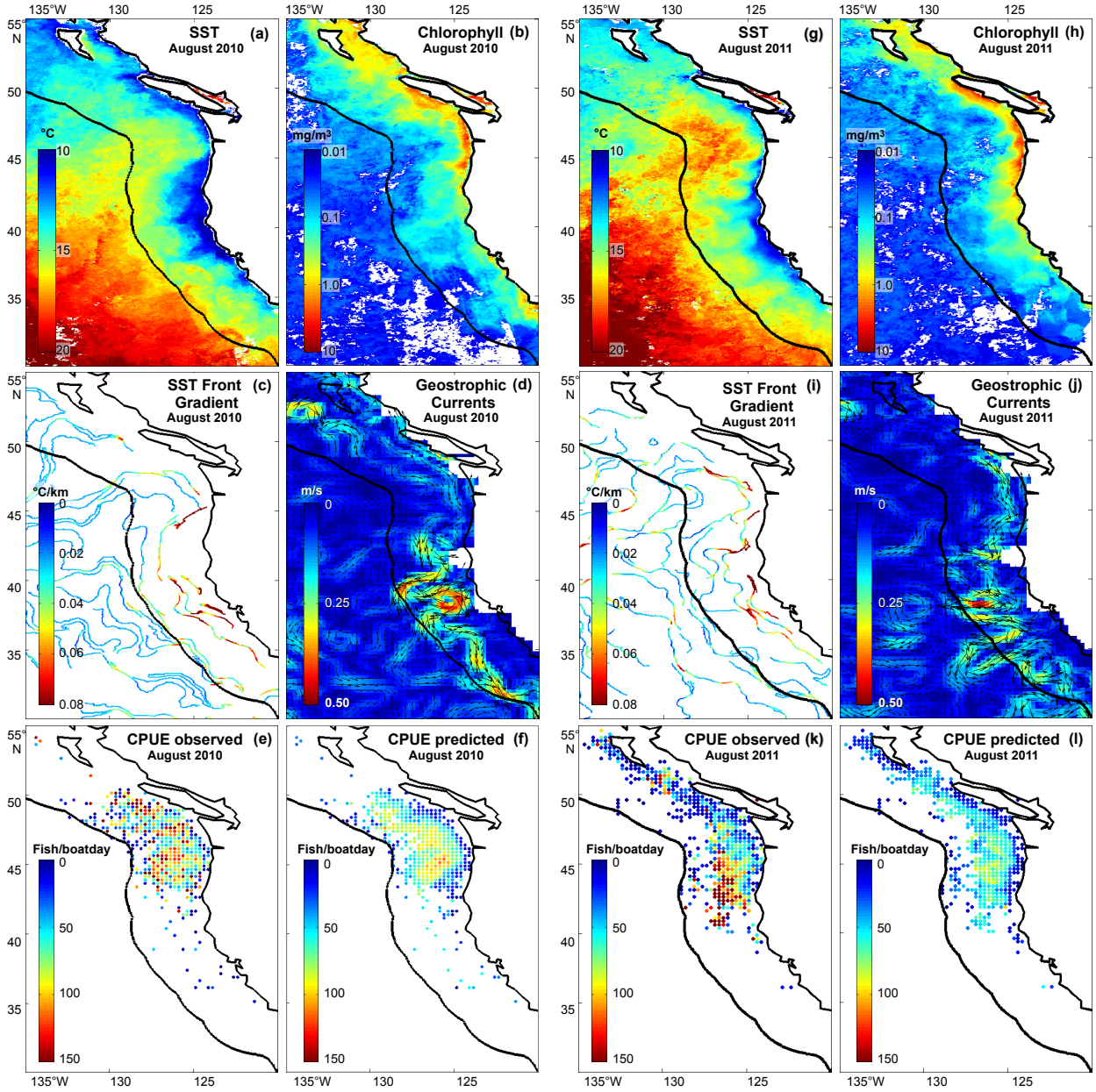
SST (a) August 2010
Chlorophyll (b) August 2010
SST (g) August 2011
Chlorophyll (h) August 2011
SST Front (c) Gradient August 2010
Geostrophic (d) Currents August 2010
SST Front (i) Gradient August 2011
Geostrophic (j) Currents August 2011
CPUE observed (e) August 2010
CPUE predicted (f) August 2010
CPUE observed (k) August 2011
CPUE predicted (l) August 2011
°C
mg/m³
°C/km
m/s
Fish/boatday
135°W
130
125
55° N
50
45
40
35

Figure 4.

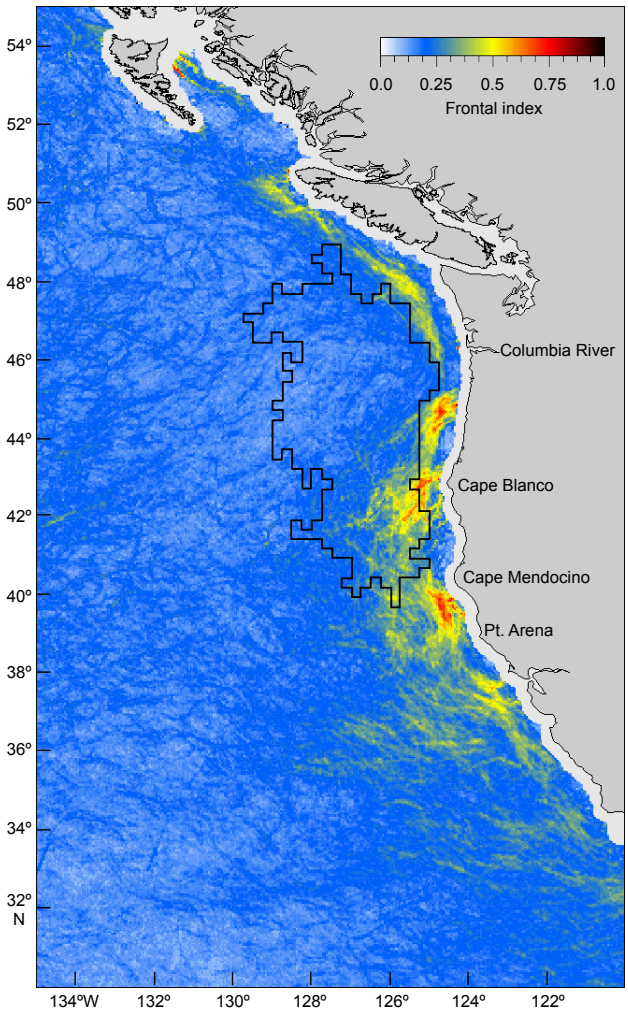
0.0 0.25 0.5 0.75 1.0
Frontal index
Columbia River
Cape Blanco
Cape Mendocino
Pt. Arena
54°
52°
50°
48°
46°
44°
42°
40°
38°
36°
34°
32°
N
134°W
132°
130°
128°
126°
124°
122°

Figure 5.

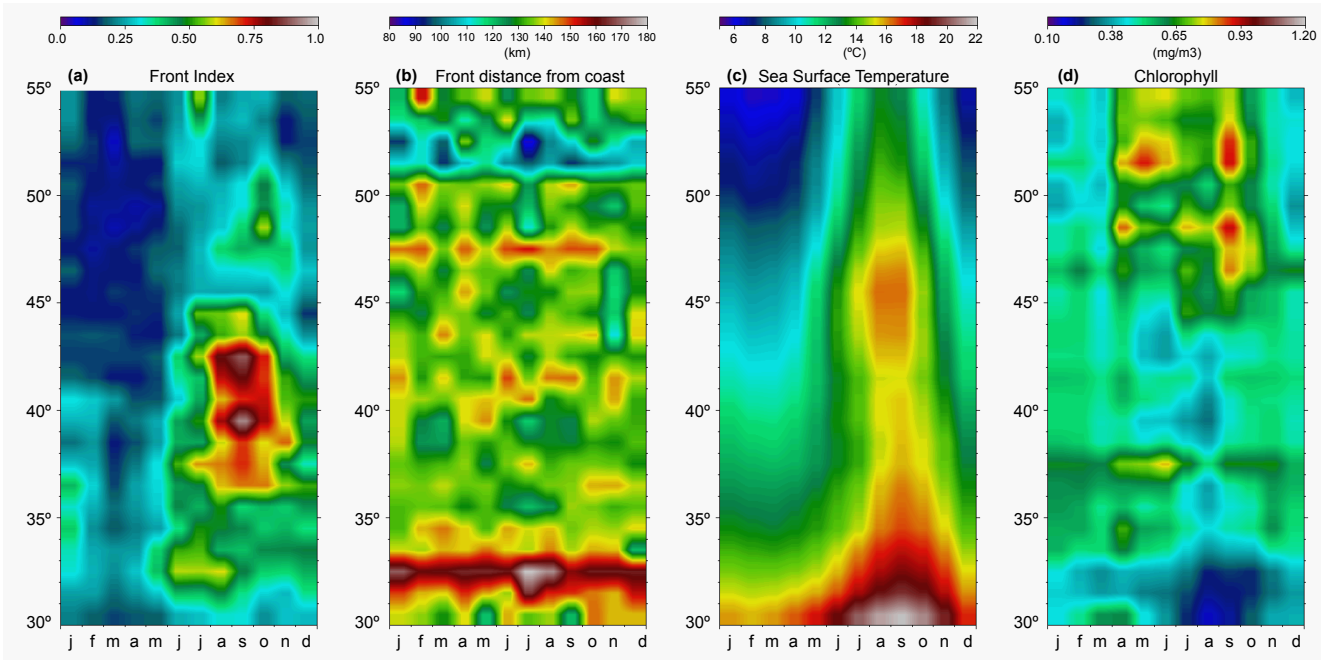
0.0 0.25 0.50 0.75 1.0
(a) Front Index
80 90 100 110 120 130 140 150 160 170 180
(km)
(b) Front distance from coast
6 8 10 12 14 16 18 20 22
(ºC)
(c) Sea Surface Temperature
0.10 0.38 0.65 0.93 1.20
(mg/m3)
(d) Chlorophyll
55º
50º
45º
40º
35º
30º
j f m a m j j a s o n d

Figure 6.

APPENDICES

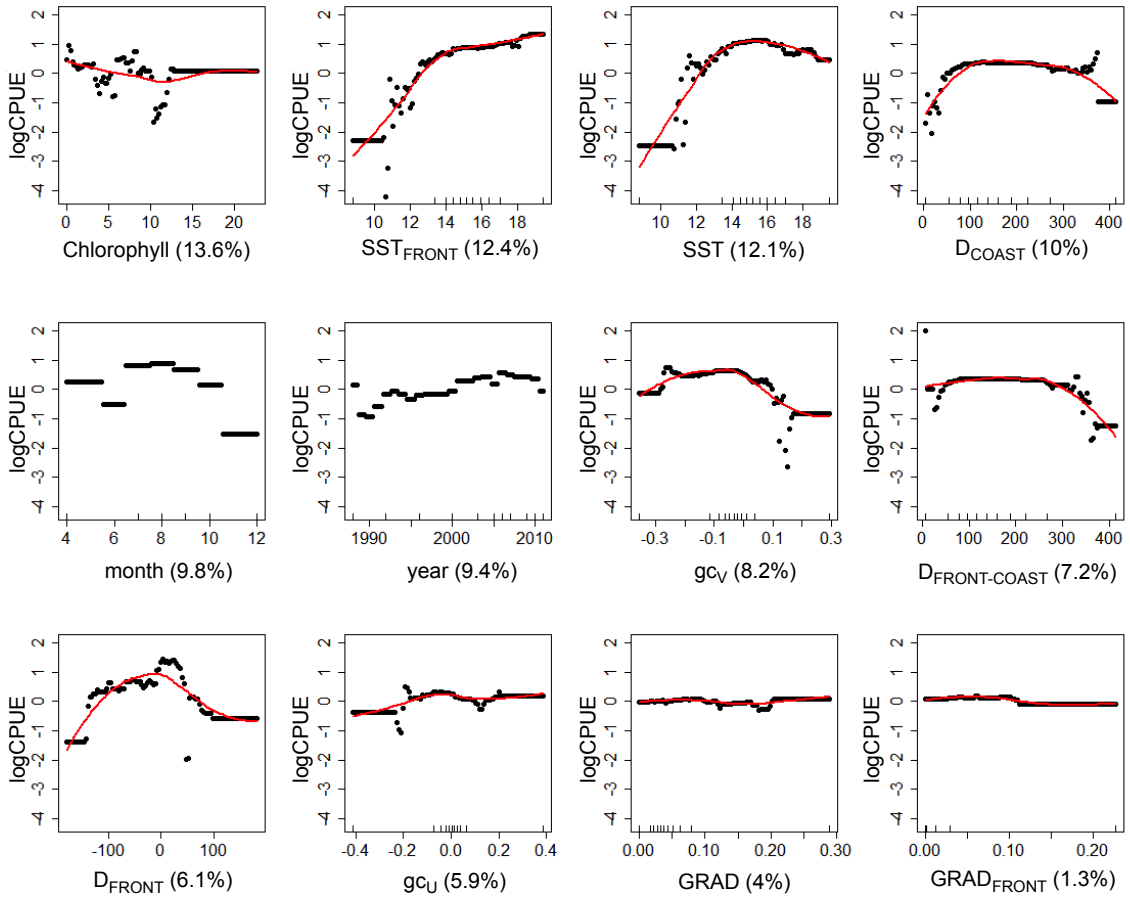

Appendix 1. Preliminary BRT model results using all predictors. BRT fitted functions of all predictors and relative percentage of contributions (33.3% total explained variance). Dots are 100 values generated by BRT model to describe the fitted function. Red line are polynomial fit curves of the dots. SST_{FRONT}, D_{COAST}, $GRAD$, and $GRAD_{FRONT}$ were dropped because of high correlation with other variables or small contribution

Appendix 2. Mean, standard deviation and coefficient of variation for total explained variance and relative contribution of all variables in both preliminary and final boosted regression tree model. Mean and SD are calculated using the leave-one-year-out analysis (N=24)

Variables	Preliminary BRT		Final BRT	
	Mean±SD %	Coeff. of Variation	Mean±SD %	Coeff. of Variation
Total explained variance	33.31 ± 1.34	0.040	31.74 ± 1.12	0.035
chlorophyll	14.06 ± 0.67	0.048	17.05 ± 0.65	0.038
SST_{FRONT}	12.46 ± 1.27	0.102	excluded	
SST	11.00 ± 0.81	0.074	18.77 ± 0.73	0.039
D_{COAST}	10.44 ± 0.78	0.075	excluded	
$D_{FRONT-COAST}$	9.46 ± 0.71	0.075	16.12 ± 0.65	0.040
gc_V	8.61 ± 0.66	0.076	9.13 ± 0.64	0.070
D_{FRONT}	7.20 ± 0.53	0.073	9.18 ± 0.74	0.081
month	6.93 ± 0.73	0.105	11.95 ± 0.72	0.060
year	6.19 ± 0.82	0.132	11.64 ± 0.97	0.083
gc_U	6.08 ± 0.50	0.083	6.15 ± 0.57	0.093
GRAD	4.59 ± 0.61	0.134	excluded	
$GRAD_{FRONT}$	2.98 ± 0.69	0.233	excluded	

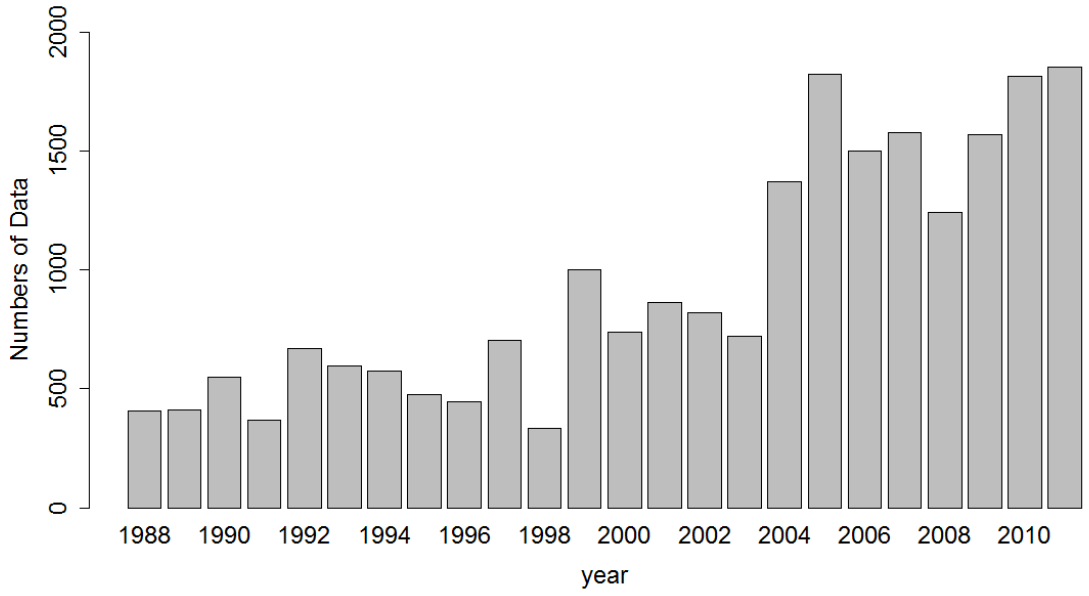

Appendix 3. Numbers of CPUE (aggregated 1/4 by 1/4 degree) data used in BRT model (from 1988 to 2011). From 1988 to 2003 only US logbook data is available, and from 2004 both US and Canadian logbook data are available. The US and Canadian CPUE abundance indices were compared and found to be similar and the US-Canadian merged index has been used in this analysis.